

Downscaled estimates of late 21st century severe weather from CCSM3

Vittorio A. Gensini · Thomas L. Mote

Received: 15 May 2014 / Accepted: 29 December 2014 / Published online: 15 January 2015
© Springer Science+Business Media Dordrecht 2015

Abstract High-resolution dynamical downscaling is used to explore 2080–2090 peak-season hazardous convective weather as simulated from the Community Climate System Model version 3. Downscaling to 4 km grid spacing is performed using the Weather Research and Forecasting model. Tornadoes, damaging wind gusts, and large hail are simulated using a model proxy at hourly intervals for locations east of the U.S. Continental Divide. Future period results are placed into context using 1980–1990 output. While a limited sample size exists, a statistically significant increase in synthetic severe weather activity is noted in March, whereas event frequency is shown to slightly increase in April, and stay the same in May. These increases are primarily found in the Mississippi, Tennessee, and Ohio River valleys. Diurnally, most of the increase in hazardous convective weather activity is shown to be in the hours surrounding local sunset. Peak-season severe weather is also shown to be more variable in the future with a skewed potential toward larger counts. Finally, modeled proxy events are compared to environmental parameters known to generate hazardous convective weather activity. These environmental conditions explain over 80 % of the variance associated with modeled reports during March–May and show an increasing future tendency. Finally, challenges associated with dynamical downscaling for purposes of resolving severe local storms are discussed.

1 Introduction

A major point of discussion in severe weather climatology surrounds the future of deep, moist convection in an anthropogenically altered climate. Historically, the record of U.S. hazardous convective weather (HCW; i.e., tornadoes, damaging wind gusts, and large hail) has been driven largely by reporting. Problems associated with the reporting process and population biases have made it difficult to determine trends from reports (see discussions in Doswell and Burgess 1988; Grazulis 1993; Brooks and Doswell 2001; Brooks and Doswell 2002; Verbout et al. 2006; and Doswell 2007).

V. A. Gensini (✉)
Meteorology Program, College of DuPage, 425 Fawell Boulevard, Glen Ellyn, IL 60327, USA
e-mail: gensiniv@cod.edu

T. L. Mote
Climatology Research Laboratory, Department of Geography, University of Georgia, 210 Field Street,
Athens, GA 30602, USA

Due to the uncertainty associated with reports, recent research has instead examined the variability of environmental conditions necessary for the formation of HCW. These studies suggest that environmental conditions related to hazardous convective weather will increase in response to elevated greenhouse forcing (Del Genio et al. 2007; Trapp et al. 2007, 2009; Marsh et al. 2009; Van Klooster and Roebber 2009; Brooks 2013; Gensini et al. 2014; Diffenbaugh et al. 2013; Allen et al. 2014). Despite the mounting environmental evidence, recent climate change assessments have largely avoided any conclusions regarding potential changes of HCW in a future climate (see discussions in Alley et al. (2007) and Karl et al. 2009). The latest Intergovernmental Panel on Climate Change (IPCC AR5) report lacks any definitive conclusions regarding extreme convective weather. This lack of confidence is primarily due to the opaque historical record of HCW reports and the inability to directly link environmental control parameters to events (Alexander and Coauthors 2013).

While Global Climate Model (GCM) output can simulate future environmental conditions favorable for the formation of HCW, the grid spacing (typically on the order of 100-km) lacks the ability to resolve processes associated with HCW. However, new research indicates that synthetic reports produced by high-resolution (4 km; hourly) regional climate models can accurately capture the spatio-temporal variability of observed reports when forced with coarse resolution GCM-scale conditions (Trapp et al. 2011; Mahoney et al. 2012; Robinson et al. 2013; Gensini and Mote 2014; Sanderson et al. 2014). Dynamical downscaling for purposes of resolving HCW events has yet to be performed on GCM-scale future projections. Thus, this is the first study to compare historical and future synthetic severe weather reports from the same GCM.

2 Background

Dynamically downscaled global reanalysis data (with an initial input horizontal grid spacing similar to many GCMs) has accurately represented HCW during the peak of the convective season (May–June; Trapp et al. 2011; Robinson et al. 2013). The Community Climate System Model version 3 (CCSM3) control run was also found to accurately portray spatial and temporal variability during March–May while correctly timing the diurnal hourly frequency of HCW (Gensini and Mote 2014). While dynamical downscaling GCM output for purposes of resolving HCW is in its infancy, these studies indicate a promising future of research.

Downscaling for HCW is recommended at a horizontal grid spacing ≤ 4 km, as severe convective storms can be permitted at this grid spacing (Weisman et al. 1997). The main challenge associated with dynamical downscaling continues to be its computationally expensive nature, though, there is little doubt this challenge will become increasingly less important in the future. However, grid spacings from the latest suite of GCM models used for the IPCC AR5 report ranged from 4° by 5° to about 1° by 1° , indicating that dynamical downscaling will likely be pertinent for years to come.

As previously discussed, one must recognize several potential pitfalls when drawing conclusions from the recorded history of HCW. Studies examining the past 30 years of HCW activity using objective methods indicate that environmental conditions (Gensini and Ashley 2011; Robinson et al. 2013) and modeled proxy reports (Robinson et al. 2013) have exhibited little to no trend, despite a significant increase in HCW reports the same period. Inflation in HCW reporting is well documented in the literature (e.g., Doswell and Burgess 1988; Grazulis 1993; Brooks and Doswell 2001, 2002; Verbout

et al. 2006; and Doswell 2007), and hence, recent increases in economic losses from severe thunderstorms (Changnon 2001) and tornadoes (Brooks and Doswell 2001; Changnon 2009) have been attributed to changes in the societal landscape (e.g., population, property value) rather than an increase in the frequency of HCW events (Bouwer 2011).

While no trends in HCW synthetic reports or environments exist over the past 30 years, several GCMs project a bullish increase in the ingredients supportive of HCW by the late 21st century (Del Genio et al. 2007; Marsh et al. 2007; Trapp et al. 2007a, 2009; Van Klooster and Roebber 2009; Diffenbaugh et al. 2013). Using dynamically downscaled data from the North American Regional Climate Change Assessment Program (NARCCAP; Mearns et al. 2009, 2012), similar increases in HCW environments were found across a large portion of the U.S. (Gensini et al. 2014) for a mid-century simulation spanning the period 2041–2065. These studies agree that projected inflation in HCW activity are largely a function of increases in convective available potential energy (CAPE), associated with augmentation in future period near-surface specific humidity values during periods when deep-layer wind shear remains adequate for organized convection.

While an environmental approach has been commonly used to this point, results herein give researchers first glances into storm-scale responses to anthropogenically altered synoptic convective environments. High-resolution dynamical downscaling for purposes of resolving HCW has yet to be performed for future period GCM scenarios, prior to the work presented here. Building from a previous historical scenario used in Gensini and Mote (2014), this study presents the first results of potential future changes in U.S. severe weather activity using synthetic reports derived from high-resolution dynamical downscaling.

3 Methodology

3.1 Model information

3.1.1 Global climate model

The CCSM3 is a coupled global climate spectral model consisting of atmosphere, land surface, sea-ice, and ocean components. CCSM3 uses an 85-wavenumber triangular truncation grid spacing (approximately 1.4° resolution at the equator) in the horizontal, and has 26 levels in the vertical (Collins et al. 2006). Available output includes a control run (no changes in external climate forcing), a 20th century simulation (containing the observed changes of greenhouse gases, sulphate aerosols, volcanic aerosols, and solar irradiance from the 20th century), and 21st century scenarios (containing estimated changes in greenhouse gas and aerosol concentrations).

For the study presented here, two 11-year epochs were compared to evaluate potential changes in future HCW activity. The historical (1980–1990) and future (2080–2090) downscaled periods use data based on a simulation initialized in 1870 and simulated through the end of the 21st century. This simulation utilizes data based on the special report for emissions scenario (SRES) A2 scenario, characterized by, “a very heterogeneous world with continuously increasing global population and regionally oriented economic growth that is more fragmented and slower than in other storylines” (Nakicenovic et al. 2000). This aggressive, but not worse case, scenario is chosen in an effort to assess potential changes in HCW to atmospheric responses associated with increasing anthropogenic carbon emissions.

3.1.2 Regional climate model

Regional Climate Model (RCM) configurations were chosen following previous research downscaling CCSM3 historical fields (Gensini and Mote 2014). Thus, we again use the non-hydrostatic advanced research core of the Weather Research and Forecasting (WRF-ARW) model (Skamarock et al. 2008). Output fields from the CCSM3 at 0000 UTC on 1 March of each year are used to initialize the RCM. Integrations are then performed over a three-month period, providing CCSM3 boundary conditions to the RCM every six hours, while the first six hours of the simulation are discarded to account for model spin-up (Skamarock 2004). This longer integration time is desirable as it supports better representation of influences associated with longer-memory processes, such as soil moisture, known to influence surface fluxes in the climate system (Gensini and Mote 2014). RCM diagnostics and parameterization schemes follow those used in Gensini and Mote (2014), and are based on previous WRF-model simulations of HCW in the United States (e.g., Weisman et al. 1997; Kain et al. 2008; Trapp et al. 2011; Robinson et al. 2013).

The model-based proxy used in this research follows that used in Trapp et al. (2011) and Gensini and Mote (2014), using hourly thresholds of updraft helicity (UH) and simulated composite RADAR reflectivity factor (Z) as described by Kain et al. (2008). Specifically, a synthetic HCW event occurs when an hourly RCM grid point contains UH values $\geq 60 \text{ m}^2 \text{ s}^{-2}$ juxtaposed with Z values $\geq 40 \text{ dBZ}$ (Fig. 1). This threshold UH/Z pair has been shown to best approximate HCW activity in the U.S. during a 1980–1990 historical simulation using CCSM3 (Gensini and Mote 2014).

Synthetic HCW reports are spatially aggregated to a 50 km grid and summed to create two epoch (1980–1990; 2080–2090) climatologies for the months March–May. Based on observed HCW reports during the historical period, bias correction is applied to both historical and future periods following the method used in Gensini and Mote (2014). This is a desirable procedure when applying a downscaling framework to GCM data (Christensen et al. 2008). Finally, statistical significance was tested using the Mann–Whitney *U* test for the medians at the 95 % confidence level.

3.2 Downscaling domain

Dynamical downscaling is applied to the same study region used in Gensini and Mote (2014), and contains all points in the U.S. east of the Continental Divide. This domain contains 490,000 grid points in a Lambert Conformal Conic projection, equating to between 4 and 4.25 km grid spacing depending on latitude. Given the central Great Plains has the highest annual frequency of HCW (Brooks et al. 2003b), it is hypothesized that potential changes in HCW activity will be most prominent in this high frequency region. Changes in HCW distributions may occur outside of this region due to a changing climate, but this study is not able to address such scenarios.

4 Results

We begin with modeled proxy reports of HCW. Raw counts of synthetic HCW reveal a 27 % increase in future period events. Stratifying by month, most of this increase is found in March (increases approaching 70 %), whereas April shows a slight increase (15 %) and May remains virtually unchanged (Fig. 2). This does not necessarily imply a shift in the temporal climax of HCW; rather, a greater probability of such events earlier in the annual cycle, and thus an

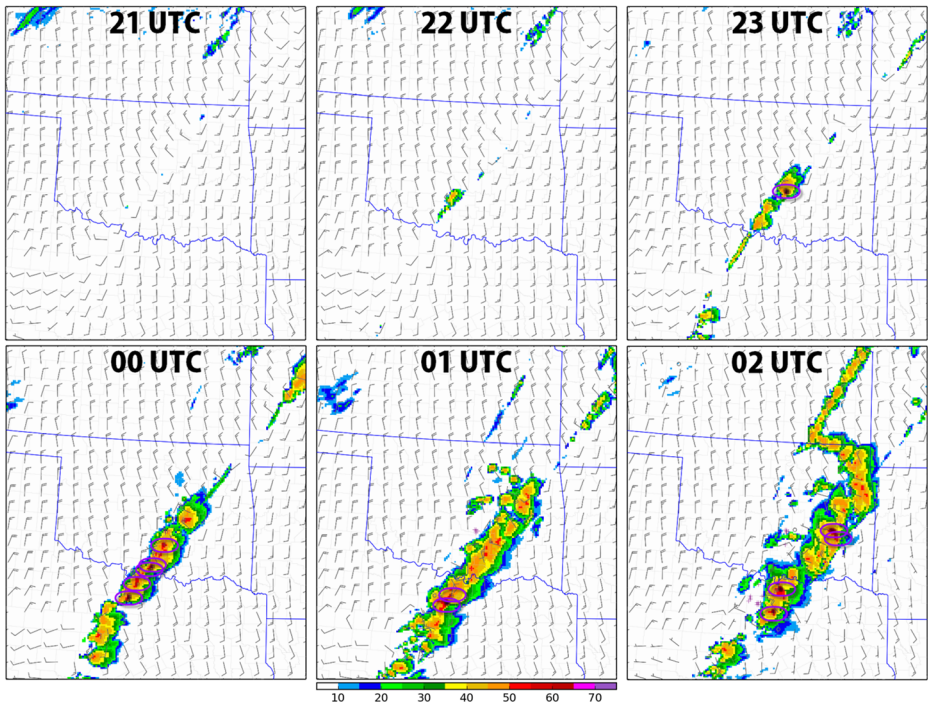


Fig. 1 Progression of RADAR composite reflectivity factor (dBZ; fill) and 10-m wind (*knots*; *wind barbs*) from 2100 UTC 2 May 2090 to 0200 UTC 3 May 2090. *Purple ovals* highlight areas of proxy-based severe convective weather reports

increase in the overall frequency is depicted. Examinations of seasonal HCW changes suggest a future increase in the variability of peak-season events, indicated by a “fanning” of the cumulative frequency through the months examined (Fig. 3). This is further shown by nearly a doubling in standard deviation (778 to 1433 synthetic reports) from the historical to future epoch and an increase in the coefficient of variation from .29 to .43 respectively. Interestingly, recent research indicates that changes in annual variability are already being noted (Brooks et al. 2014; Tippett 2014). From an environmental ingredients perspective, this variability is primarily a function of adequate deep-layer wind shear juxtapositioning with CAPE. Consequently, increases in peak-season HCW variability suggest that synoptic scale controls, such as jet-stream location, are likely to be different in a future climate. This variability is broadly consistent with recent research relating arctic amplification with mid-latitude weather extremes (Francis and Vavrus 2012; Petoukhov et al. 2013; Screen and Simmonds 2013) due to a decline in Arctic sea-ice cover (Francis et al. 2009).

Similar to Gensini and Mote (2014), severe weather reports from the Storm Prediction Center’s severe weather database (Schaefer and Edwards 1999) were used to provide a simple bias correction factor to historical and future period proxy reports (Fig. 2), a necessary procedure when downscaling GCM data (Christensen et al. 2008). These corrections do not affect the fractional changes across epochs; they instead adjust the absolute magnitudes of change into a context consistent with historical observed HCW reports. It should be noted that observed HCW reports, in particular, are a challenge to bias correct due to the nature of the reporting process. Lastly, modeled HCW reports are inherently biased toward the supercell spectrum of convective

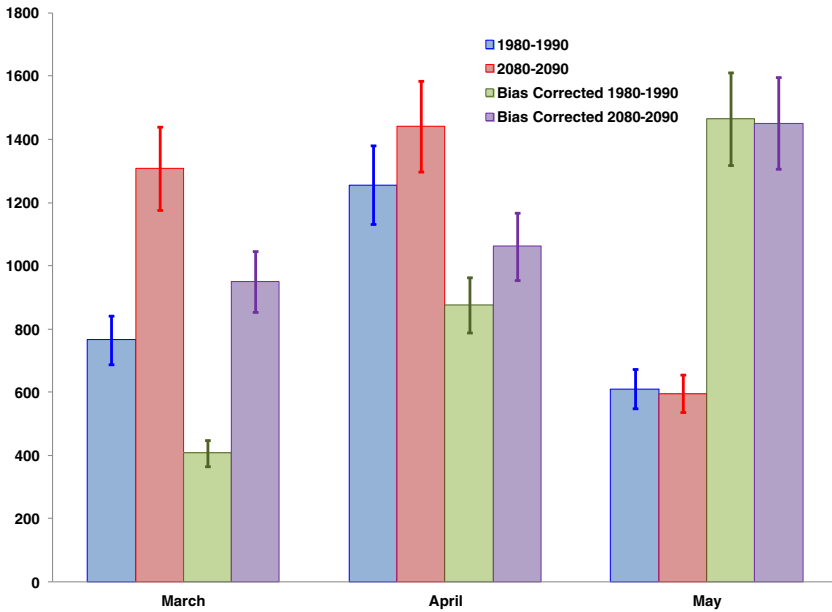


Fig. 2 Average monthly comparisons of raw and bias corrected synthetic severe weather reports. *Error bars* indicate the standard error

mode due to the 4 km grid spacing of the RCM. The use of UH would conceptually trigger more supercell events (due to the associated size of a mesocyclone relative to the horizontal grid spacing used) versus events produced by other convective modes (e.g., squall lines).

Spatially, the largest increases in future period HCW are depicted across the Middle Mississippi, Lower Mississippi, Ohio, and Tennessee River valleys (Fig. 4). In these regions, results indicate increases of 2–8+ HCW reports per season on average. Some isolated points in and close to these regions depicted a statistically significant decrease. For example, a relative cluster of notable decrease in HCW activity is shown across Florida in this simulation. However, these statistically significant decreases (23 grid cells) are largely outweighed by roughly 6.5 times more grid cells that illustrated a statistically significant increase across the domain. Diurnally, the largest HCW frequency increases were found from 2100 to 0500 UTC (Fig. 5), which coincides with the typical maximum in HCW across the U.S. (Kelly et al. 1978).

Next, we focus on modeled composite reflectivity. While not a hazard itself, it can be used as a surrogate to gauge updraft and storm intensity. This is not a new process as meteorologists routinely use RADAR reflectivity to operationally imply storm intensity (Lemon 1977), objectively track thunderstorm echoes (Dixon and Wiener 1993; Johnson et al. 1998; Han et al. 2009) and classify potential hail size (Witt et al. 1998). The composite reflectivity value of 50 dBZ was chosen due its documented ability to discriminate for severe hail events when used with melting layer height (Donavon and Jungbluth 2007) and was again aggregated to a 50 km grid for comparison.

Significant increases in future period 50 dBZ values were found during the months of March and April, while May showed no significant change (Fig. 6). Most of the increases in March are identified in the southeast Great Plains through the southern and southeastern U.S., northward through the Mississippi and Ohio River valleys (Fig. 7). By April, a majority of the increase has shifted northward into the Ohio River valley, consistent with the northward

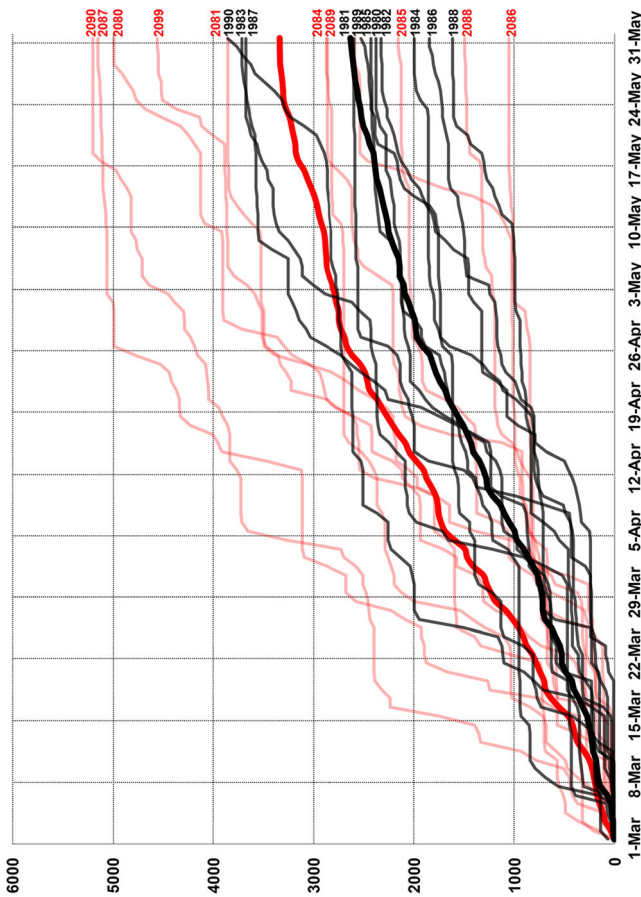


Fig. 3 Cumulative frequency of historical (*black*) and future (*red*) period synthetic hazardous convective weather reports. Thick *black* and *red* lines indicate averages for their respective period

climatological shift of severe weather as the season progresses (Brooks et al. 2003a; Gensini and Ashley 2011). Results herein suggest that late-century, early-season thunderstorms will be of greater frequency, likely a function of robust increases in CAPE and near-surface specific humidity depicted by several GCMs and RCMs (Del Genio et al. 2007; Trapp et al. 2007a, 2009; Van Klooster and Roebber 2009; Diffenbaugh et al. 2013; Gensini et al. 2014).

We conclude with a discussion of environmental control parameters known to favor deep convection, specifically CAPE and 0–6-km bulk wind difference (BWD). An average increase of 236 % is shown across all months of future period average frequencies of grid points with CAPE exceeding 2000 J kg^{-1} (Fig. 8). This robust increase in CAPE is consistent with recent studies examining ensembles of GCM output for convective purposes (Del Genio et al. 2007; Trapp et al. 2007a, 2009; Diffenbaugh et al. 2013) during March–May. In addition, the product of CAPE and 0–6 km BWD has been widely used to discriminate potential significant severe weather environments for climatological purposes due to its ease of calculation (Brooks et al. 2003b). The calculation used herein follows the proximity Craven-Brooks composite methodology of Gensini and Ashley (2011), restricting events to CAPE values exceeding 100 J kg^{-1} . Similar to the synthetic HCW report distribution, the number of grid points with

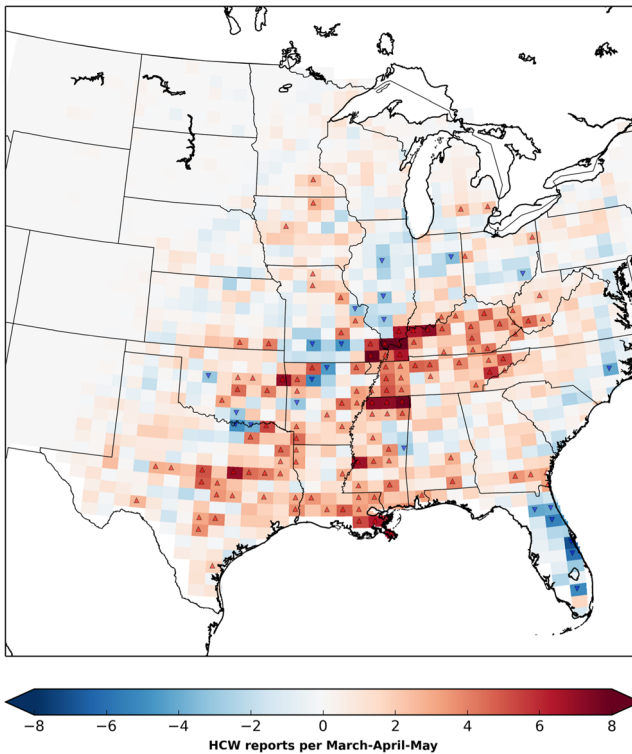


Fig. 4 Average difference between 2080–2090 and 1980–1990 modeled severe weather reports. Red (blue) grid cells indicate a positive (negative) change in the average number of modeled reports per season. *Triangles* indicate statistical significance at the 95 % confidence level

a product of CAPE and 0–6 km BWD exceeding 20,000 show a significant increase in March and April, with no meaningful change in May (Fig. 9). There are only a few distinguishable spatial shifts in the distribution of CAPE (Fig. 10a, b) and significant severe weather environments (Fig. 10c, 10d) over the epochs examined. Rather, an overall general increase is noted from the historical to the future period.

These results are corroborated by the agreement between large-scale instability/shear parameters and modeled HCW reports. The product of CAPE and 0–6 km BWD exceeding 20,000 explains 81 % of the variability associated with HCW reports over the historical and future periods examined (Fig. 11). This supports recent research depicting the ability of high-resolution dynamical downscaling to replicate large-scale conditions forcing interannual and sub-seasonal variability in HCW activity (Gensini and Mote 2014). This result is significant, as one of the main weaknesses in environmental analysis is the inability to discuss changes on the storm-scale. It appears, however, that environmental analysis is an efficient predictor of HCW occurrence across the domain and study periods analyzed.

5 Summary and conclusions

This study is the first to use dynamical downscaling for purposes of examining potential changes in hazardous convective weather under a business-as-usual emissions scenario. Using

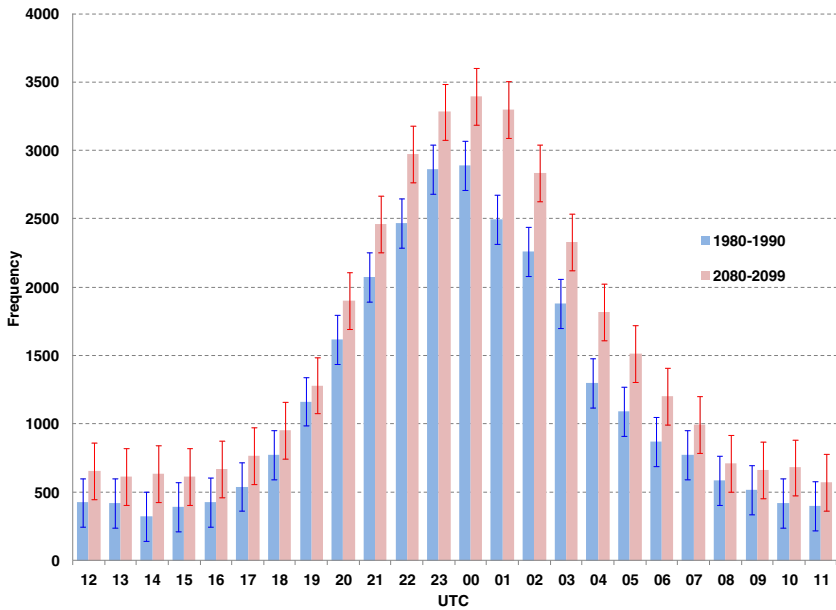


Fig. 5 Diurnal frequency comparison of historical (blue) and future (red) severe weather reports. Error bars indicate the standard error

data from the Community Climate System Model version 3 downscaled by the Weather Research and Forecasting model, an artificial report proxy consisting of downscaled 2–5 km

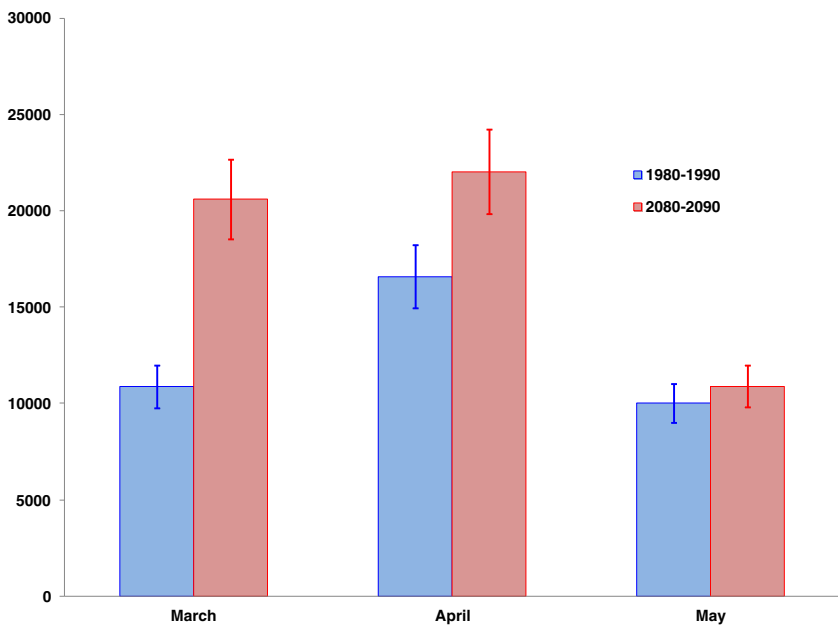


Fig. 6 Average monthly comparisons of historical and future period grid cell counts with modeled composite reflectivity ($Z \geq 50$ dBZ). Error bars indicate the standard error

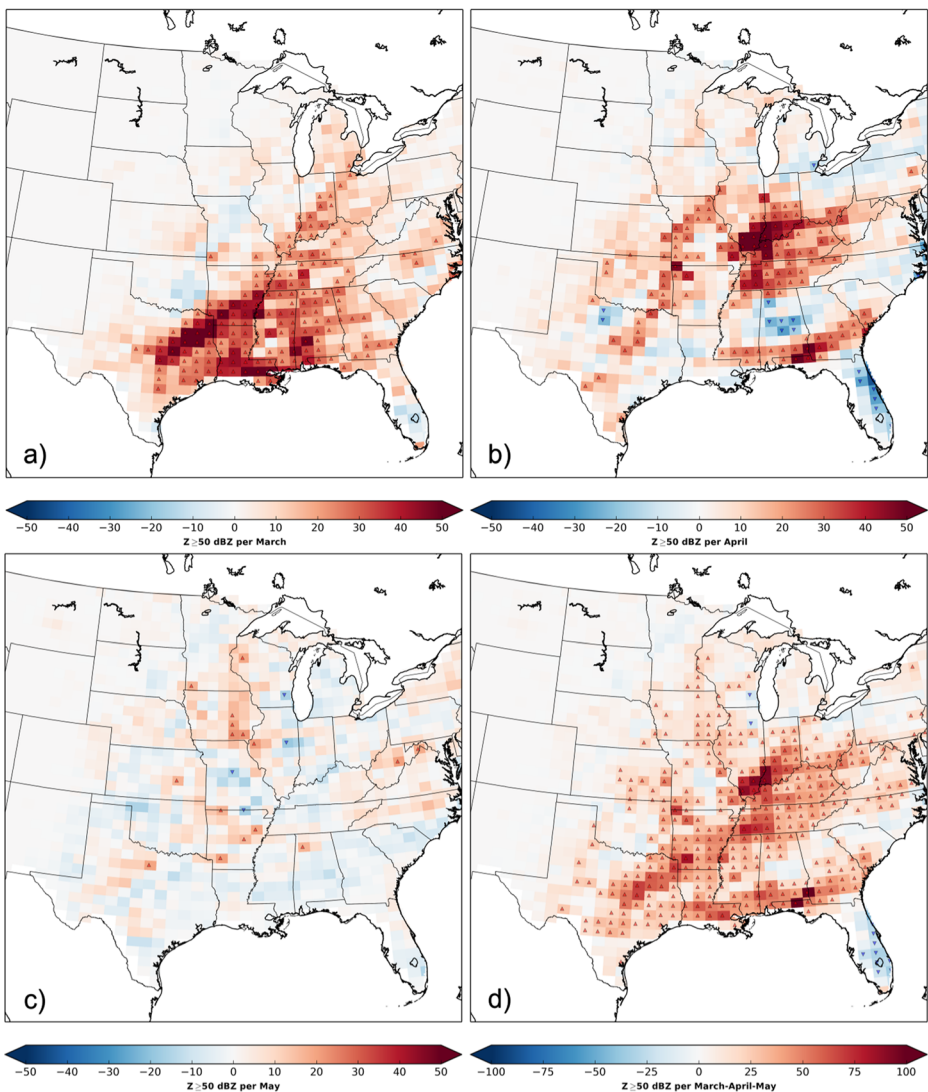


Fig. 7 Average difference between 2080–2090 and 1980–1990 modeled composite reflectivity values ≥ 50 dBZ for March (a), April (b), May (c), and March–May (d). Red (blue) grid cells indicate a positive (negative) change in the average number of modeled reports per season. Triangles indicate statistical significance at the 95 % confidence level

updraft helicity and RADAR composite reflectivity factor was used to simulate occurrences of tornadoes, damaging wind gusts, and large hail at hourly intervals over the eastern two-thirds of the U.S. during a historical (1980–1990) and future (2080–2090) period. Using observed severe weather reports to bias correct, a significant future increase in hazardous convective weather frequency and variability is revealed, especially during the afternoon hours during the months of March and April. The largest increase in future severe weather events is found across the Middle Mississippi, Lower Mississippi, Ohio, and Tennessee River valleys, with an overall frequency increase of 27 %. Thus, this region would be poised to receive an additional 2–8+

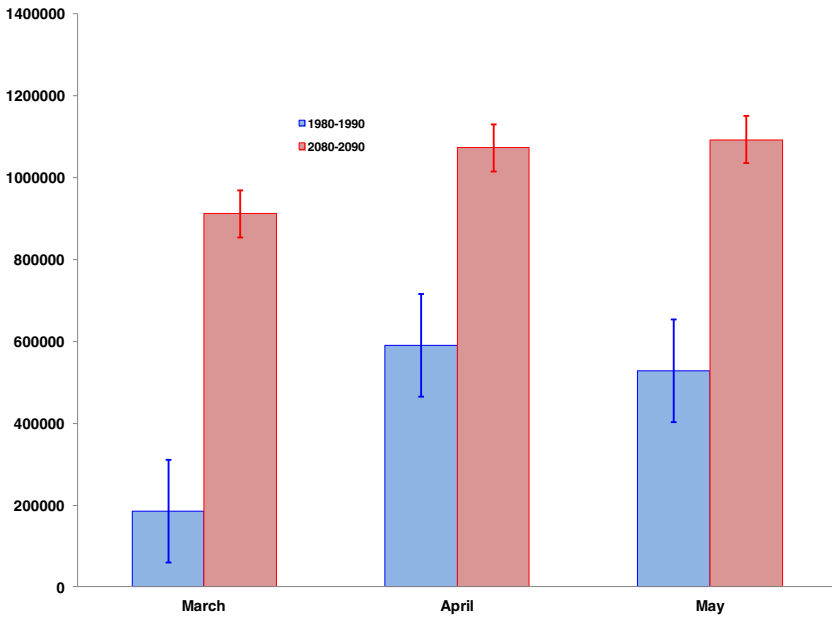


Fig. 8 As in Fig. 4.6, but for grid cell counts with $CAPE \geq 2000 \text{ J kg}^{-1}$

severe weather reports per 50 km grid box during March–May. In addition, modeled composite reflectivity, a surrogate for storm occurrence, is shown to significantly increase across a large portion of the analyzed domain, again specifically during the months of March and April.

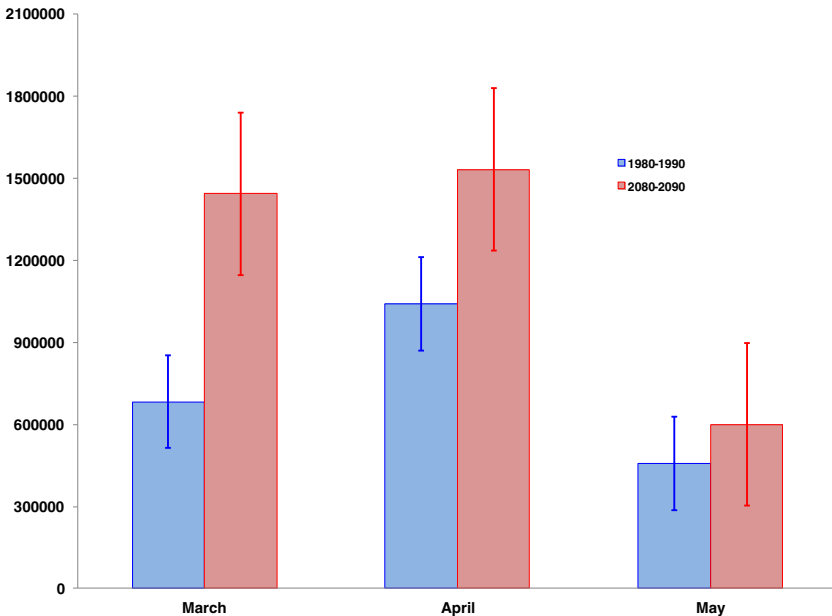


Fig. 9 As in Fig. 4.6, but for grid cell counts with $CAPE \times 0\text{--}6\text{-km BWD} \geq 20,000$ with $CAPE \geq 100 \text{ J kg}^{-1}$

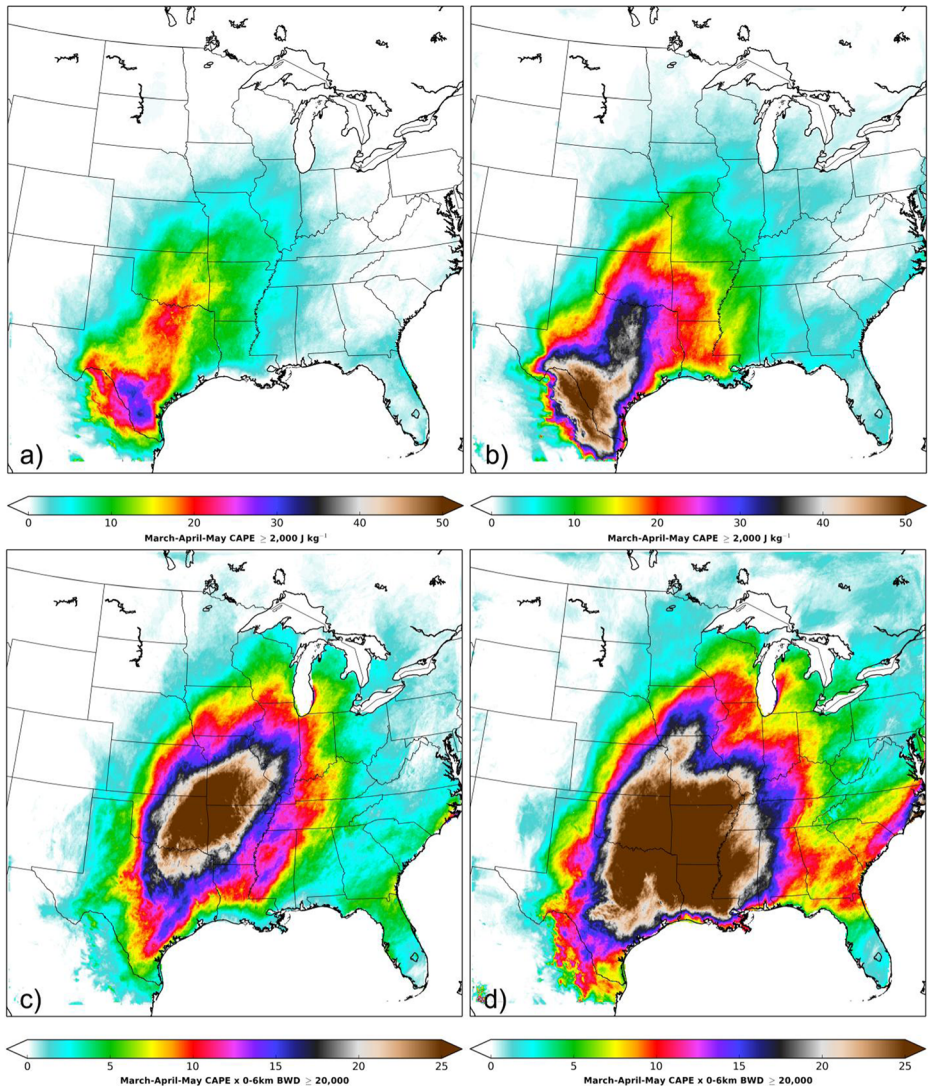


Fig. 10 Average frequency of March–May historical (a) $\text{CAPE} \geq 2000 \text{ J kg}^{-1}$ and (b) the product of CAPE and 0–6-km BWD exceeding 20,000. Panels (c) and (d) represent the future period respectively. In the case of $\text{CAPE} \times 0\text{--}6\text{-km BWD} \geq 20,000$, CAPE is constrained to only evaluate events with $\geq 100 \text{ J kg}^{-1}$

These results, along with a quickly growing body of literature, suggest that late-century thunderstorms will be of greater intensity/frequency, likely a function of robust increases in CAPE and near-surface specific humidity depicted by several GCMs and RCMs (Del Genio et al. 2007; Trapp et al. 2007a, 2009; Van Klooster and Roebber 2009; Diffenbaugh et al. 2013; Gensini et al. 2014; Allen et al. 2014). These previous studies are solidified by results presented herein, as large-scale environmental controls such as CAPE and deep-layer wind shear are shown to explain over 80 % of the variability in modeled severe weather reports.

The main obstacle for this particular study is dataset length. Due to the computationally expensive nature of dynamical downscaling, it was only feasible to examine two ten-year

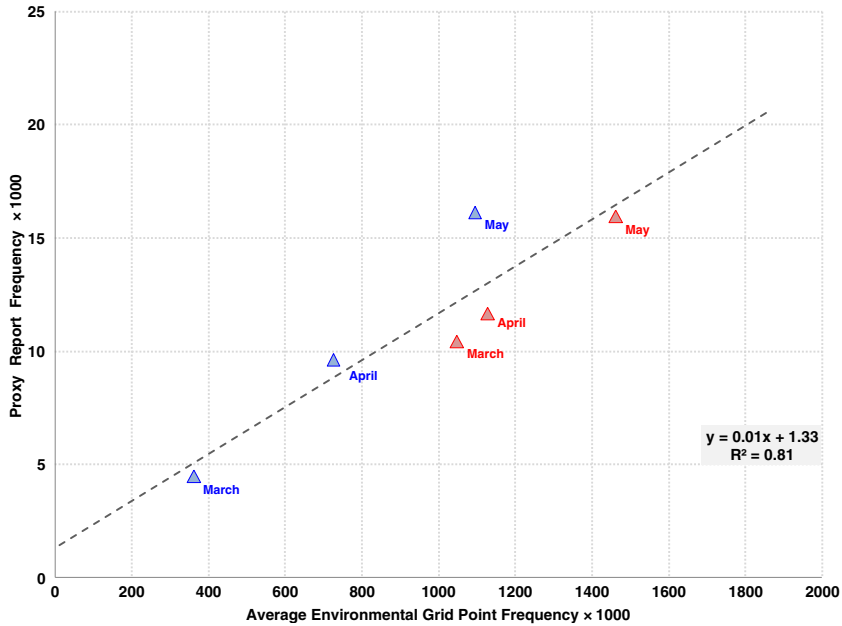


Fig. 11 Linear correlation between average grid point frequency with $\text{CAPE} \times 0\text{--}6\text{-km BWD} \geq 20,000$ and average synthetic report frequency by month. *Blue triangles* correspond to the period 1980–1990, while *red triangles* correspond to the period 2080–2090. The least-squares regression equation and coefficient of determination are displayed in the *gray box*

periods. Ultimately, a multi-model ensemble approach over a period of 30 years would be most desirable for this type of study, and accordingly, we are limited with our ability to make definitive conclusions regarding severe weather in the late 21st century. However, this study expands an existing body of literature indicating the potential for future increases in severe convective weather (Del Genio et al. 2007; Trapp et al. 2007a, 2009; Van Klooster and Roebber 2009; Diffenbaugh et al. 2013; Gensini et al. 2014; Allen et al. 2014). Overall, dynamical downscaling for purposes of resolving mesoscale phenomenon, such as severe local storms, continues to emerge as an admirable methodological technique for climate change assessments.

Acknowledgments The authors would like to thank three anonymous reviewers that provided comments resulting in a significantly enhanced manuscript. In addition, thanks to Drs. Harold Brooks (National Severe Storms Laboratory) and Marshall Shepherd (University of Georgia) for feedback during initial stages of this research.

References

- Alexander L, and Coauthors (2013) Climate change 2013: the physical science basis. Contribution of Working Group I to the Fifth Assessment Report of the Intergovernmental Panel on Climate Change
- Allen JT, Karoly DJ, Walsh KJ (2014) Future Australian severe thunderstorm environments. Part II: the influence of a strongly warming climate on convective environments. *J Climate* 27:3848–3868

- Alley R, and Coauthors (2007) Summary for policymakers. *Climate Change 2007: The Physical Science Basis*, S. Solomon, and Coauthors, Eds., Cambridge University Press, 1–18
- Bouwer LM (2011) Have disaster losses increased due to anthropogenic climate change? *Bull Am Meteorol Soc* 92:39–46
- Brooks HE (2013) Severe thunderstorms and climate change. *Atmos Res* 123:129–138
- Brooks HE, Doswell CA III (2001) Normalized damage from major tornadoes in the United States: 1890–1999. *Weather Forecast* 16:168–176
- Brooks HE, Doswell CA III (2002) Deaths in the 3 May 1999 Oklahoma City tornado from a historical perspective. *Weather Forecast* 17:354–361
- Brooks HE, Doswell CA III, Kay MP (2003a) Climatological estimates of local daily tornado probability for the United States. *Weather Forecast* 18:626–640
- Brooks HE, Lee JW, Craven JP (2003b) The spatial distribution of severe thunderstorm and tornado environments from global reanalysis data. *Atmos Res* 67–68:73–94
- Brooks HE, Carbin GW, Marsh PT (2014) Increased variability of tornado occurrence in the United States. *Science* 346:349–352
- Changnon SA (2001) Damaging thunderstorm activity in the United States. *Bull Am Meteorol Soc* 82:597–608
- Changnon SA (2009) Tornado losses in the United States. *Nat Hazards Rev* 10:145–150
- Christensen JH, Boberg F, Christensen OB, Lucas-Picher P (2008) On the need for bias correction of regional climate change projections of temperature and precipitation. *Geophys Res Lett* 35:L20709
- Collins WD, Bitz CM, Blackmon ML, Bonan GB, Bretherton CS, Carton JA, Smith RD (2006) The community climate system model version 3 (CCSM3). *J Clim* 19(11):2122–2143. <http://journals.ametsoc.org/doi/pdf/10.1175/JCLI3761.1>
- Del Genio AD, Yao M-S, Jonas J (2007) Will moist convection be stronger in a warmer climate? *Geophys Res Lett* 34:L16703
- Diffenbaugh NS, Scherer M, Trapp RJ (2013) Robust increases in severe thunderstorm environments in response to greenhouse forcing. *Proc Natl Acad Sci* 110:16361–16366
- Dixon M, Wiener G (1993) TITAN: thunderstorm identification, tracking, analysis, and nowcasting—a radar-based methodology. *J Atmos Oceanic Tech* 10:785–797
- Donavon RA, Jungbluth KA (2007) Evaluation of a technique for radar identification of large hail across the Upper Midwest and Central Plains of the United States. *Weather Forecast* 22:244–254
- Doswell CA III (2007) Small sample size and data quality issues illustrated using tornado occurrence data. *Electron J Sev Storms Meteorol* 2:1–16
- Doswell CA III, Burgess DW (1988) On some issues of United States tornado climatology. *Mon Weather Rev* 116:495–501
- Francis JA, Vavrus SJ (2012) Evidence linking Arctic amplification to extreme weather in mid-latitudes. *Geophys Res Lett* 39:L06801
- Francis JA, Chan W, Leathers DJ, Miller JR, Veron DE (2009) Winter Northern Hemisphere weather patterns remember summer Arctic sea-ice extent. *Geophys Res Lett* 36:L07503
- Gensini VA, Ashley WS (2011) Climatology of potentially severe convective environments from the North American Regional Reanalysis. *Electron J Sev Storms Meteorol* 6:1–40
- Gensini VA, Mote TL (2014) Estimations of hazardous convective weather in the U.S. using dynamical downscaling. *J Climate* 27:6581–6598
- Gensini VA, Ramseyer C, Mote TL (2014) Future convective environments using NARCCAP. *Int J Climatol* 34:1699–1705
- Grazulis TP (1993) Significant tornadoes: 1680–1991. *Environmental Films*, 1326 pp
- Han L, Fu S, Zhao L, Zheng Y, Wang H, Lin Y (2009) 3D convective storm identification, tracking, and forecasting—An enhanced TITAN algorithm. *J Atmos Oceanic Tech* 26:719–732
- Johnson J, MacKeen PL, Witt A, Mitchell EDW, Stumpf GJ, Eilts MD, Thomas KW (1998) The storm cell identification and tracking algorithm: An enhanced WSR-88D algorithm. *Weather Forecast* 13:263–276
- Kain JS, and Coauthors (2008) Some practical considerations regarding horizontal resolution in the first generation of operational convection-allowing NWP. *Weather Forecast* 23:931–952
- Karl TR, Melillo JM, and Peterson TC (2009) *Global climate change impacts in the United States*. Cambridge University Press
- Kelly DL, Schaefer JT, McNulty RP, Doswell CA III, Abbey RF Jr (1978) An augmented tornado climatology. *Mon Weather Rev* 106:1172–1183
- Lemon LR (1977) New severe thunderstorm radar identification techniques and warning criteria (No. AWS-TR-77-271). Air weather service scott AFB IL. <http://oai.dtic.mil/oai/oai?verb=getRecord&metadataPrefix=html&identifier=ADA099510>
- Mahoney K, Alexander MA, Thompson G, Barsugli JJ, Scott JD (2012) Changes in hail and flood risk in high-resolution simulations over Colorado's mountains. *Nat Clim Chang* 2:125–131

- Marsh PT, Brooks HE, Karoly DJ (2007) Assessment of the severe weather environment in North America simulated by a global climate model. *Atmos Sci Lett* 8:100–106
- Marsh PT, Brooks HE, Karoly DJ (2009) Preliminary investigation into the severe thunderstorm environment of Europe simulated by the Community Climate System Model 3. *Atmos Res* 93:607–618
- Mearns LO, and Coauthors (2012) The North American regional climate change assessment program: overview of phase I results. *Bull Am Meteorol Soc* 93:1337–1362
- Mearns LO, Gutowski W, Jones R, Leung R, McGinnis S, Nunes A, Qian Y (2009) A regional climate change assessment program for North America. *EOS Trans Am Geophys Union* 90:311
- Nakicenovic N, and Coauthors (2000) Special report on emissions scenarios: a special report of Working Group III of the Intergovernmental Panel on Climate Change, 599 pp
- Petoukhov V, Rahmstorf S, Petri S, Schellnhuber HJ (2013) Quasiresonant amplification of planetary waves and recent Northern Hemisphere weather extremes. *Proc Natl Acad Sci* 110:5336–5341
- Robinson ED, Trapp RJ, Baldwin ME (2013) The geospatial and temporal distributions of severe thunderstorms from high-resolution dynamical downscaling. *J Appl Meteorol Climatol* 52:2147–2161
- Sanderson MG, Hand WH, Groenemeijer P, Boorman PM, Webb JDC, McColl LJ (2014) Projected changes in hailstorms during the 21st century over the UK. *Int J Climatol* 35(1):15–24
- Schafer JT, and Edwards R (1999) The SPC tornado/severe thunderstorm database. 11th Conference on Applied Climatology, American Meteorological Society, 603–606
- Screen JA, Simmonds I (2013) Exploring links between Arctic amplification and mid-latitude weather. *Geophys Res Lett* 40:959–964
- Skamarock WC (2004) Evaluating mesoscale NWP models using kinetic energy spectra. *Mon Weather Rev* 132: 3019–3032
- Skamarock WC, Klemp JB, Dudhia J, Gill DO, Barker DM, Wang W, and Powers JG (2008) A description of the Advanced Research WRF version 3. NCAR Tech. Note NCAR/TN-475+STR, 113pp
- Tippett MK (2014) Changing volatility of US annual tornado reports. *Geophys Res Lett* 41:6956–6961
- Trapp RJ, Diffenbaugh NS, Brooks HE, Baldwin ME, Robinson ED, Pal JS (2007a) Changes in severe thunderstorm environment frequency during the 21st century caused by anthropogenically enhanced global radiative forcing. *Proceedings of the National Academy of Sciences* 104:19719–19723
- Trapp RJ, Diffenbaugh NS, Gluhovsky A (2009) Transient response of severe thunderstorm forcing to elevated greenhouse gas concentrations. *Geophys Res Lett* 36:L01703
- Trapp RJ, Robinson E, Baldwin M, Diffenbaugh N, Schwedler B (2011) Regional climate of hazardous convective weather through high-resolution dynamical downscaling. *Climate Dynam* 37:677–688
- Van Klooster SL, Roebber PJ (2009) Surface-based convective potential in the contiguous United States in a business-as-usual future climate. *J Climate* 22:3317–3330
- Verbout SM, Brooks HE, Leslie LM, Schultz DM (2006) Evolution of the U.S. tornado database: 1954–2003. *Weather Forecast* 21:86–93
- Weisman ML, Skamarock WC, Klemp JB (1997) The resolution dependence of explicitly modeled convective systems. *Mon Weather Rev* 125:527–548
- Witt A, Eilts MD, Stumpf GJ, Johnson J, Mitchell EDW, Thomas KW (1998) An enhanced hail detection algorithm for the WSR-88D. *Weather Forecast* 13:286–303